N-Type Organic Semiconductors Based on π-Deficient Pentacenequinones: Synthesis, Electronic Structures, Molecular Packing, and Thin Film Transistors

Zhixiong Liang,[†] Qin Tang,[†] Jing Liu,[†] Jinhua Li,[§] Feng Yan,[§] and Qian Miao*[,†,‡,⊥]

[†]*Department of Chemistry, and* [‡]*Center of Novel Functional Molecules, the Chinese University of Hong Kong, Shatin, New Territories, Hong Kong, China,* [§]*Department of Applied Physics, the Hong Kong Polytechnic University, Hung Hom, Kowloon, Hong Kong, China, and* [⊥]*Institute of Molecular Functional Materials* (*Areas of Excellence Scheme, University Grants Committee*), *Hong Kong, China*

Quinones are well-known as organic oxidizing reagents in organic synthesis and biological systems, but their ability of accepting electrons was rarely explored in connection with n-type organic semiconductors. Here, we report a comprehensive study on two groups of π-deficient pentacenequinones, fluorinated pentacenequinones and *N*-heteropentacenequinones, highlighting their electronic structures, molecular packing, and n-channel thin film transistors. It is found that replacing H atoms of pentacenequinone with F atoms or replacing C atoms with N can lower the lowest unoccupied molecular orbital (LUMO) energy level of pentacenequinone to yield n-type organic semiconductors with the field effect mobility up to higher than $0.1 \, cm^2 V^{-1} s^{-1}$ in thin film transistors. A comparison between the two groups of quinones in terms of their electronic structures and molecular packing has led to interesting findings on the roles of electron-withdrawing moieties in tuning frontier molecular orbitals and π-stacking. Another interesting finding on the molecular packing is the quadruple weak hydrogen bonds, which link the neighboring π-stacks of quinones. This study suggests that π-deficient quinones would be a general design for n-type organic semiconductors.

Introduction

Pentacene has led small-molecule organic semiconductors as a benchmark for applications in thin film transistors, and functionalized pentacenes have been extensively studied, for organic semiconductors with improved properties and better understanding of the structure–property relationship.[1] Similar to pentacene, pentacenequinones are rigid and planar molecules. They are known as the synthetic precursors for pentacene and functionalized pentacenes but were almost unexplored for applications in organic electronic devices as active components. For example, 6,13-pentacenequinone (**1** in Figure 1) is an insulator[2] and is also known as a major impurity in pentacene.[3] Quinones are well-known as

organic oxidizing reagents in organic synthesis and biological systems, but their ability of accepting electrons was rarely explored in connection with n-type organic semiconductors.[4] Following our recent success in applying 5,7,12,14-tetraaza-6,13-pentacenequinone (**5** in Figure 1) as an n-type semiconductor in thin film transistors,[5] we have investigated π-deficient pentacenequinones as a general design for n-type organic semiconductors. The π-deficient pentacenequinones studied here are assorted into two groups, fluorinated pentacenequinones (**2, 3**) and *N*-heteropentacenequinones (**4**−**7**), as shown in Figure 1. It is found that both of the two groups of molecules function as n-type organic semiconductors in thin film transistors with the electron mobility up to higher than $0.1 \, cm^2 V^{-1} s^{-1}$. Detailed below are the synthesis, electronic structures, molecular packing, and n-channel thin film transistors of these π-deficient pentacenequinones.

A general strategy of obtaining n-type organic semiconductors is adding electron-withdrawing groups, such as fluorine or cyano or imide moieties, to a known (p-type) semiconducting molecule in order to lower the lowest

*To whom correspondence should be addressed. E-mail: miaoqian@cuhk.edu.hk.

(1) For recent reviews, see: (a) Murphy, A. R.; Fréchet, J. M. *Chem. Rev.* **2007,** *107,* 1066–1096. (b) Anthony, J. E. *Chem. Rev.* **2006,** *106,* 5028–5048. (c) Anthony, J. E. *Angew. Chem., Int. Ed.* **2008,** *47,* 452–483. (d) Bendikov, M.; Wudl, F.; Perepichka, D. F. *Chem. Rev.* **2004,** *104,* 4891–4945.

(2) (a) Jurchescu, O. D.; Popinciuc, M.; van Wees, B. J.; Palstra, T. T. M. *Adv. Mater.* **2007,** *19,* 688–692. (b) Parisse, P.; Picozzi, S.; Ottaviano, L. *Org. Electron.* **2007,** *8,* 498–504. (c) Li, Z.; Du, J.; Tang, Q.; Wang, F.; Xu, J.; Yu, J. C.; Miao, Q. *Adv. Mater.* **2010,** *22,* 3242–3246.

(3) (a) Jurchescu, O. D.; Baas, J.; Palstra, T. T. M. *Appl. Phys. Lett.* **2004,** *84,* 3061. (b) Roberson, L. B.; Kowalik, J.; Tolbert, L. M.; Kloc, C.; Zeis, R.; Chi, X.; Fleming, R.; Wilkins, C. *J. Am. Chem. Soc.* **2005,** *127,* 3069–3075.

(4) For n-type organic semiconductors based on anthraquinone, see: (a) Mamada, M.; Nishida, J.; Tokito, S.; Yamashita, Y. *Chem. Commun.* **2009,** 2177–2179. (b) Mamada, M.; Kumaki, D.; Nishida, J.; Tokito, S.; Yamashita, Y. *ACS Appl. Mater. Interfaces* **2010,** *2,* 1303–1307.

(5) Tang, Q.; Liang, Z.; Liu, J.; Xu, J.; Miao, Q. *Chem. Commun.* **2010,** *46,* 2977–2979.

Article

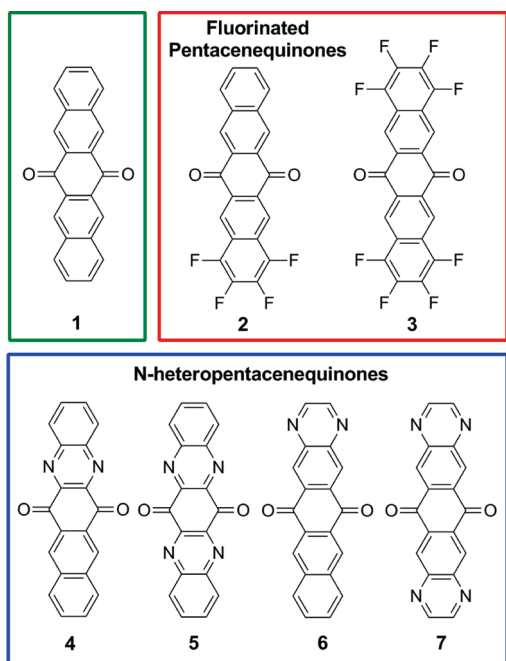*Chem. Mater., Vol. 22, No. 23, 2010* **6439**

Figure 1. Structures of pentacenequinones.

unoccupied molecular orbital (LUMO) energy level.[6] The π-deficient pentacenequinones studied here feature two types of electron-withdrawing moieties, namely, fluorine atoms and pyrazine-type nitrogen atoms. Fluorination is a useful strategy to convert a p-type organic semiconductor to an n-type one by lowering the energy level of LUMO without great change of the molecular shape and size.[7] Fluorinated pentacenes have been reported as n-type organic semiconductors with good electron mobility.[8] Fluorinated pentacenequinones **2** and **3** were synthesized as the precursors for the partially fluorinated

pentacenes[9,10] but were not recognized as organic semiconductors themselves. *N*-Heteropentacenequinones are oxidation products of *N*-heteropentacenes. Although N-rich heteropentacenes are predicted as n-type organic semiconductors,[11,12] to the best of our knowledge, all the semiconductors based on *N*-heteropentacenes that have been reported up to date are p-type,[13] possibly due to the difficulty in synthesis[14] and low stability of N-rich heteropentacenes.[15] The *N*-heteropentacenequinones shown in Figure 1 have highly related structures and, thus, are logical subjects for studying the structure−property relationship. Among them, **6** and **7** are new compounds, and **5** has been recently studied by us for application in organic electronic devices.[5] Although **4** was reported decades ago,[16] it was not fully characterized, and this study appears for the first time for its application in organic electronic devices being explored.

The electronic structure and the molecular assembly of organic semiconductors in the solid state are two key factors that determine their performance in organic electronic devices. In general, good electronic performance requires strong electronic coupling between neighboring molecules in the solid.[1b] As indicated by the theoretical investigations by Brédas and co-workers, one of the major parameters governing the charge transport properties at the microscopic level is the amplitude of the electronic transfer integrals between adjacent semiconductor molecules, and the transfer integrals depend on both the relative positions of the interacting molecules and the shape (bonding−antibonding pattern) of their frontier molecular orbitals.[17] Therefore, in this study, the two groups of quinones are compared in terms of their electronic structures and molecular packing to better understand the roles of the two electron-withdrawing moieties.

Results and Discussion

Synthesis. As detailed in the Supporting Information, fluorinated pentacenequiones **2** and **3** were synthesized starting from tetrafluorophthalic acid following the reported methods.[9] Shown in Scheme 1 are the syntheses of *N*-heteropentacenequinones **4−7** with two different strategies, oxidation of the corresponding *N*-heteropentacenes and the Diels−Alder reaction. **4** and **5** were prepared by oxidizing 5,14-dihydro-5,14-diazapentacene and 5,14-dihydro-5,7,12,14-tetraazapentacene, respectively, with $K_2Cr_2O_7$ in acidic conditions. Particularly, **4** was yielded as a ~2:1 mixture with **8** in a yield of 51%, and it was successfully separated by dissolving **8** in trifluoroacetic acid (isolated yields of **4** and **8** were 19% and 6%,

(6) For reviews on n-type organic semiconductors and n-channel organic thin film transistors, see: (a) Newman, C. R.; Frisbie, C. D.; da Silva Filho, D. A.; Brédas, J.-L.; Ewbank, P. C.; Mann, K. R. *Chem. Mater.* **2004**, *16*, 4436−4451. (b) Zaumseil, J.; Sirringhaus, H. *Chem. Rev.* **2007**, *107*, 1296−1323. (c) Yamashita, Y *Chem. Lett.* **2009**, *38*, 870−875. (d) Anthony, J. E.; Facchetti, A.; Heeney, M.; Marder, S. R.; Zhan, X. *Adv. Mater.* **2010**, *22*, 3876−3892.
(7) (a) Yoon, M.-H.; Facchetti, A.; Stern, C. E.; Marks, T. J. *J. Am. Chem. Soc.* **2008**, *128*, 5792−5801. (b) Facchetti, A.; Yoon, M.-H.; Stern, C. L.; Katz, H. E.; Marks, T. J. *Angew. Chem., Int. Ed.* **2003**, *42*, 3900−3903.
(8) (a) Sakamoto, Y.; Suzuki, T.; Kobayashi, M.; Gao, Y.; Fukai, Y.; Inoue, Y.; Sato, F.; Tokito, S. *J. Am. Chem. Soc.* **2004**, *126*, 8138−8140. (b) Tang, M. L.; Oh, J. H.; Reichardt, A. D.; Bao, Z. *J. Am. Chem. Soc.* **2009**, *131*, 3733−3740.
(9) Miao, Q. Ph.D. Dissertation. Columbia University, NewYork, 2005.
(10) Swartz, C. R.; Parkin, S. R.; Bullock, J. E.; Anthony, J. E.; Mayer, A. C.; Malliaras, G. G. *Org. Lett.* **2005**, *7*, 3163−3166.
(11) Winkler, M.; Houk, K. N. *J. Am. Chem. Soc.* **2007**, *129*, 1805−1815.
(12) Miao, S.; Appleton, A. L.; Berger, N.; Barlow, S.; Marder, S. R.; Hardcastle, K. I.; Bunz, U. H. F. *Chem.—Eur. J.* **2009**, *15*, 4990−4993.
(13) (a) Miao, Q.; Nguyen, T.-Q.; Someya, T.; Blanchet, G. B.; Nuckolls, C. *J. Am. Chem. Soc.* **2003**, *125*, 10284−10287. (b) Tang, Q.; Zhang, D.; Wang, S.; Ke, N.; Xu, J.; Yu, J. C.; Miao, Q. *Chem. Mater.* **2009**, *21*, 1400−1405. (c) Tang, Q.; Liu, J.; Chan, H. S.; Miao, Q. *Chem.—Eur. J.* **2009**, *15*, 3965−3969. (d) Weng, S.-Z.; Shukla, P.; Kuo, M.-Y.; Chang, Y.-C.; Sheu, H.-S.; Chao, I.; Tao, Y.-T. *ACS Appl. Mater. Interfaces* **2009**, *1*, 2071−2079. (e) Ma, Y.; Sun, Y.; Liu, Y.; Gao, J.; Chen, S.; Sun, X.; Qiu, W.; Yu, G.; Cui, G.; Hu, W.; Zhu, D. *J. Mater. Chem.* **2005**, *15*, 4894−4898.

(14) Barashenkov, G. G.; Fedoryak, D. M. *Ukr. Khim.* **2007**, *73*, 108−111.
(15) Wu, J. I.; Wannere, C. S.; Mo, Y.; Schleyer, P. v. R.; Bunz, U. H. F. *J. Org. Chem.* **2009**, *74*, 4343−4349.
(16) Wittig, G.; Harle, H.; Knauss, E.; Niethammer, K. *Chem. Ber.* **1960**, 951−962.
(17) (a) Brédas, J.-L.; Calbert, J. P.; da Silva, D. A.; Cornil, J. *Proc. Natl. Acad. Sci. U.S.A.* **2002**, *99*, 5804−5809. (b) Brédas, J.-L.; Beljonne, D.; Coropceanu, V.; Cornil, J. *Chem. Rev.* **2004**, *104*, 4931−5003.
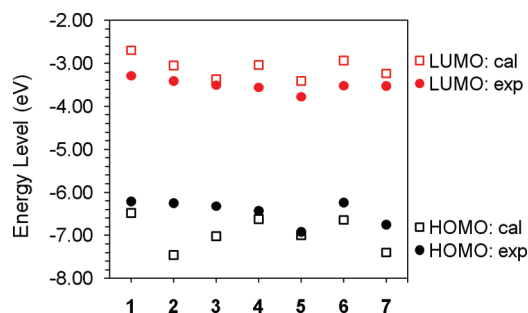
Table 1. Reduction Potentials, Absorption Edge, and Frontier Orbital Energy Levels of Pentacenequinones

compound	$E_{red}^{1/2}$ vs Fc$^+$/Fc (V)	absorption edge (nm)	LUMO (eV)	HOMO (eV)	optical gap (eV)
1	−1.51	425	−3.29	−6.21	2.92
2	−1.39	436	−3.41	−6.25	2.84
3	−1.29	442	−3.51	−6.32	2.81
4	−1.24	432	−3.56	−6.43	2.87
5	−1.02	395	−3.78	−6.92	3.15
6	−1.28	456	−3.52	−6.24	2.72
7	−1.27	384	−3.53	−6.75	3.22

respectively). It appeared difficult to distinguish **4** and **8** from their ^{1}H NMR spectra because NMR spectra were not available for the two compounds in the previous reports.[16,18] The structures of **4** and **8** were finally determined on the basis of the crystal structure of 6,13-bis-(triisopropylsilylethynyl)-5,14-dihydro-5,14-diazapentacene, a derivative of **4**.[19] The syntheses of **6** and **7** were achieved using Diels−Alder reactions, in which the corresponding quinone was the dienophile and the diene was generated in situ from α,α,α′,α′-tetrabromo-*o*-dimethyl-pyrazine at Cava's condition,[20] followed by elimination of HBr.[21] All the π-pentacenequinones are yellow crystalline powders, which appear stable to ambient air and light and do not decompose with heating up to 300 °C.

Electronic Structures. The electronic structures of **1**−**7** were studied using both experimental and computational methods. Cyclic voltammograms (shown in the Supporting Information) of all the pentacenequinones in *N*,*N*-dimethylformamide (DMF) exhibited reduction waves but not oxidation waves in the testing window. The LUMO energy level of each quinone was estimated from the half-wave reduction potential vs ferrocenium/ferrocene.[22] The highest occupied molecular orbital (HOMO)−LUMO gap was determined on the basis of the absorption edge in the UV−vis absorption spectrum from a solution in DMF, and the energy level of HOMO was calculated from the LUMO energy level and optical gap. As summarized in Table 1, all the π-deficient pentacenequinones (**2**−**7**) have lower energy levels of LUMO than **1** has and also have lower HOMO energy levels than **1** has. Molecule **5**, the *N*-heteropentacenequinone with two pyrazine rings directly bonded to carbonyl groups, has the lowest LUMO energy level. Similar to **1**, **2**−**7** generally have weak absorption in the range of visible light and relatively large optical HOMO−LUMO gaps. Among the π-deficient quinones, **2**, **4**, and **6** have one π-deficient ring while **3**, **5**, and **7** have two π-deficient rings. An interesting

Scheme 1. Syntheses of *N*-Heteropentacenequinones

observation from Table 1 is that the drop of LUMO energy level upon the introduction of the first π-deficient ring (from **1** to **2**, **4**, and **6**) is generally greater than that due to the introduction of the second π-deficient ring (from **2**, **4**, and **6** to **3**, **5**, and **7**, respectively). This suggests that the second π-deficient ring has a smaller effect on lowering the LUMO energy level than the first one has.

The frontier molecular orbitals of **1**−**7** were also calculated using the hybrid density functional method B3LYP with a 6-311G** basis set. The calculated energy levels are compared with the experimental values in Figure 2. The calculated LUMO energy levels of **1**−**7** are generally in good agreement with the experimental values while the difference between the calculated and experimental values of HOMO energy level varies in a larger range. This is possibly because the experimental value of HOMO energy level was not directly measured from oxidation waves in cyclic voltammograms but estimated from the optical HOMO−LUMO gap and the LUMO energy level. As depicted graphically in Figure 3, all of the quinones have delocalized electron distribution in the LUMOs. The LUMOs of fluorinated pentacenequinones **2** and **3** show almost the same shape as that of **1** with the fluorine atoms almost not sharing the LUMO electrons. In contrast, *N*-heteropentacenequinones **4**−**7** have LUMOs

(18) Leete, E.; Ekechukwu, O.; Delvigs, P. *J. Org. Chem.* **1966**, *31*, 3734−3739.
(19) The synthesis of this derivative from **4** and its crystal structure will be reported elsewhere.
(20) Cava, M. P.; Napier, D. R. *J. Am. Chem. Soc.* **1957**, *79*, 1701−1705.
(21) For examples of synthesis of pentacenequinones using this strategy, see: (a) Bénard, C. P.; Geng, Z.; Heuft, M. A.; VanCrey, K.; Fallis, A. G. *J. Org. Chem.* **2007**, *72*, 7229−7236. (b) Okamoto, T.; Bao, Z. *J. Am. Chem. Soc.* **2007**, *129*, 10308−10309. (c) Plunkett, K. N.; Godula, K.; Nuckolls, C.; Tremblay, N.; Whalley, A. C.; Xiao, S. *Org. Lett.* **2009**, *11*, 2225−2228. (d) Hou, Y.; Wan, P. *Can. J. Chem.* **2007**, *85*, 1023−1032. (e) Ref 10.
(22) The commonly used HOMO energy level of ferrocene is −4.80 eV. See: (a) Pommerehne, J.; Vestweber, H.; Guss, W.; Mahrt, R. F.; Bässler, H.; Porsch, M.; Daub, J. *Adv. Mater.* **1995**, *7*, 551−554. (b) D'Andrade, B. W.; Datta, S.; Forrest, S. R.; Djurovich, P.; Polikarpov, E.; Thompson, M. E. *Org. Electron.* **2005**, *6*, 11−20.

Figure 2. HOMO and LUMO energy levels of **1−7** as calculated (cal) and estimated from experimental values (exp).
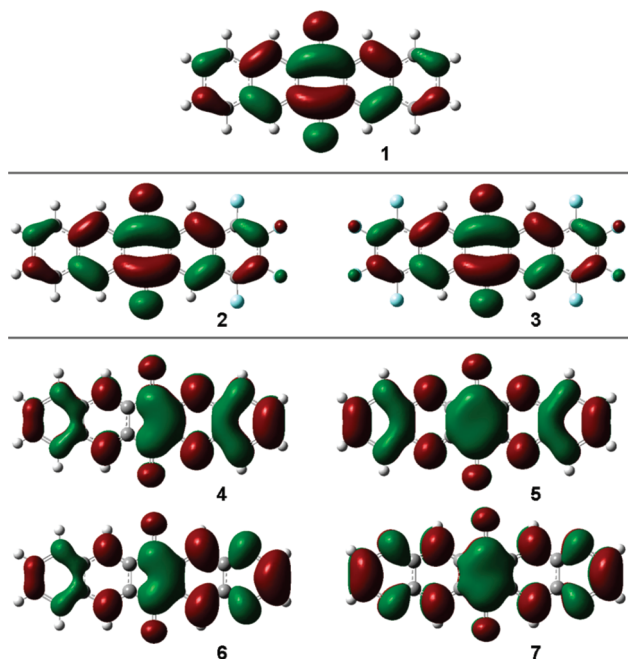

Figure 3. Calculated LUMOs of pentacenequinones showing the distribution of the positive and negative LCAO (linear combination of atomic orbitals) coefficients in red and green, respectively.

of a different pattern. This can be related to the fact that the electron-withdrawing effects of fluorine atom and pyrazine-type nitrogen atom are through induction and resonance, respectively. Although **2**, **4**, and **6** have the π-deficient ring on only one side of the molecule, the LUMOs of **2**, **4**, and **6** are relatively symmetrically distributed among the five rings.

Molecular Packing. Besides electronic structures, molecular assembly in the solid state is another key factor governing the performance of organic semiconductors. One important question in the research of organic field effect transistors is how the charge transport depends on the molecular packing of organic semiconductors.[23] Semiconducting π-molecules usually adopt two common packing motifs in the solid state: (1) herringbone packing, in which the aromatic edge-to-face interaction dominates and (2) face-to-face π-stacking, typically with some degree of displacement along the molecular axes. The theoretical investigations by Brédas and co-workers[17]
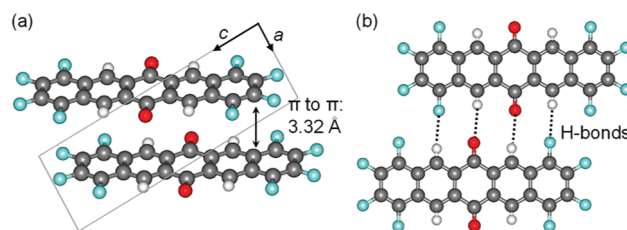
Figure 4. Crystal structure of **3**: (a) $\pi-\pi$ stacking as viewed along the *b* axis of unit cell; (b) C−H⋯O/F hydrogen bonds as shown with dashed lines.

have shown that the displacements along the long and short axes of π-stacked semiconductor molecules do strongly affect the intermolecular electronic couplings, in a way that intimately depends on the phase and nodal properties of the frontier molecular orbitals. Merely enhancing "spatial overlap" between conjugated molecules without proper control of displacements along molecular axes may not lead to strong intermolecular electronic couplings. These theoretical analyses suggest that fine-tuning of molecular packing with control of displacements along the molecular axes becomes an important task for better understanding the relationship between molecular packing and charge transport. Therefore, the following study on molecular packing of π-deficient pentacenequinones not only shows π-stacking but also highlights the relative shifts of π-stacked quinones along the molecular axes. Another interesting finding on the molecular packing is the quadruple weak hydrogen bonds,[24] which link the neighboring π-stacks of the π-deficient pentacenequinones. Although the C−H⋯O hydrogen bonds are known for benzoquinones,[24,25] the quadruple weak hydrogen bonds found in the crystal structures of π-deficient pentacenequinones are unusual.[26]

Single crystals of the π-deficient pentacenequinones were grown using the physical vapor transport technique.[27] X-ray crystallographic analysis has revealed the molecular packing of **3**, **5**, and **7**. The crystal structure of **5** was recently reported by us,[5] and the crystal structures of **3** and **7** are detailed below. As shown in Figure 4, the molecular packing of **3** features $\pi-\pi$ stacking and weak C−H⋯O/F hydrogen bonds. Molecules of **3** form infinite one-dimensional stacks with a $\pi-\pi$ distance of 3.32 Å, which is slightly shorter than the interplanar distance in graphite (3.35 Å). Such close π-stacks are accompanied with intermolecular contacts shorter than the sum of van der Waals radii not only within a stack but also between neighboring stacks. As shown in Figure 4b, the short contacts between the neighboring stacks are quadruple

(23) Coropceanu, V.; Cornil, J.; da Silva Filho, D. A.; Olivier, Y.; Silbey, R.; Bredas, J.-L. *Chem. Rev.* **2007**, *107*(4), 926–952.

(24) Desiraju, G. R. ; Steiner, T. *The Weak Hydrogen Bond in Structural Chemistry and Biology*; Oxford University Press, Oxford, 1999.

(25) Desiraju, G. R. *Crystal Engineering: The Design of Organic Solids*; Elsevier, Amsterdam, 1989; Chapter 5.

(26) The quadruple weak hydrogen bonds are also found in the reported crystal structures of 1,6,11-triaza-5,12-tetracenequinone derivatives but were not recognized in that report. See: Kim, Y.-S.; Park, S.-Y.; Lee, H.-J.; Suh, M.-E.; Schollmeyer, D.; Lee, C.-O. *Bioorg. Med. Chem.* **2003**, *11*, 1709–1714.

(27) (a) Laudise, R. A.; Kloc, C.; Simpkins, P. G.; Siegrist, T. *J. Cryst. Growth* **1998**, *187*, 449–454. (b) Buurma, A. J. C.; Jurchescu, O. D.; Shokaryev, I.; Baas, J.; Meetsma, A.; de Wijs, G. A.; de Groot, R. A.; Palstra, T. T. M. *J. Phys. Chem. C* **2007**, *111*, 3486–3489.
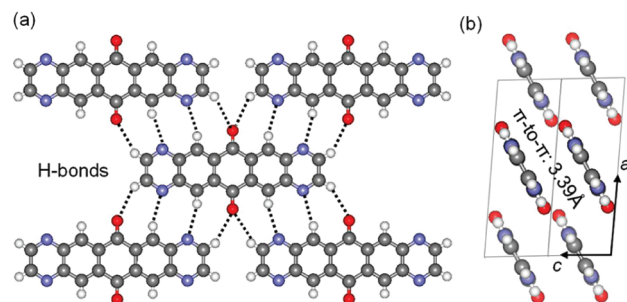
Figure 5. Crystal structure of **7**: (a) C−H···O/N hydrogen bonds as shown with dashed lines; (b) π−π stacking as viewed along the *b* axis of unit cell.

Figure 6. Relative shifts of π-stacked molecules along the long molecular axis and short molecular axis for **3**, **5**, and **7**.

weak C−H···O/F hydrogen bonds with a self-complementary ADAD-DADA pattern (D is hydrogen donor, and A is hydrogen acceptor). In these quadruple weak hydrogen bonds, the H···F and H···O distances are essentially the same and measured as 2.50 Å, and the C−H···F and C−H···O angles are 171.9° and 170.7°, respectively.

Shown in Figure 5 is the crystal structure of **7**, which features infinite one-dimensional stacks with a π−π distance of 3.39 Å and quadruple weak C−H···N/O hydrogen bonds. The neighboring stacks are linked by quadruple weak C−H···F/O hydrogen bonds with a self-complementary ADAD-DADA pattern (D is hydrogen donor, and A is hydrogen acceptor). In these quadruple weak hydrogen bonds, the H···N and H···O distances are 2.59 and 2.69 Å, respectively, and the C−H···N and C−H···O angles are 160.4° and 144.9°, respectively. Similar multiple weak hydrogen bonds were also predicted for N-rich heteropentacenes.[11] In comparison, molecules of **5**, the isomer of **7**, form infinite stacks in two directions with a π−π distance of 3.37 Å. The crystal structure of **5** also shows similar π−π stacking and quadruple weak hydrogen bonds, but the quadruple weak hydrogen bonds between molecules of **5** are of a DDAA-AADD pattern and have longer H···N distances (2.69 Å).[5] The fact that molecules of **7** stack in one direction while molecules of **5** stack in two directions is possibly related to the different patterns of weak hydrogen bonds between the neighboring stacks.

Shown in Figure 6 are the relative shifts of π-stacked molecules along the molecular axes for **3**, **5**, and **7**, clearly indicating the different effects of fluorine atoms and pyrazine-type nitrogen atoms on finely tuning π-stacking. The top molecule of **3** shifts approximately by one benzene ring along both the long molecule axis and the short molecular axis. Such arrangement can be understood in terms of overlapping between positively charged atoms (C that is bonded to F or O) and negatively charged atoms (F and C that is bonded to H). In comparison, the relative shifts of π-stacked molecules along molecular axes are much smaller in the crystals of **5** and **7**. As shown in Figure 6b, the top molecule of **5** shifts over the bottom molecule along the short molecule axis by 1.95 Å and shifts along the long axis by only 0.21 Å. As shown in Figure 6c, molecules of **7** have slightly smaller shifts
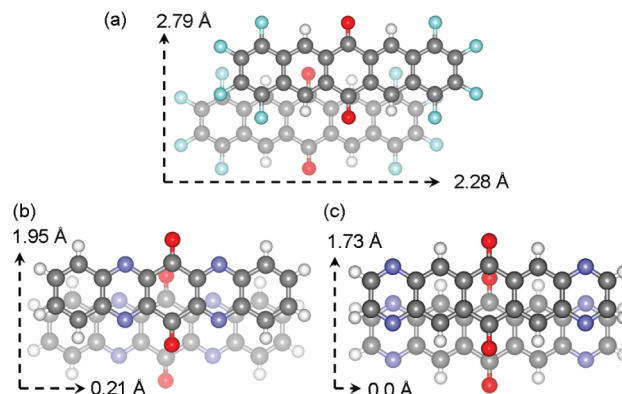
(by about 0.2 Å) along both the short and long molecular axis. Particularly, there is no shift along the long molecular axis between two stacked molecules of **7**.

Thin Film Transistors. The best way to study the structure−property relationship of organic semiconductors is to relate the structure features with the electrical properties measured from single crystal devices because the variation of thin film crystallinity, morphology, and grain boundary has dramatic effects on charge transport and can be avoided using a single crystal device. Unfortunately, the single crystals of π-deficient pentacenequinones grown in this study were not suitable for fabrication of single crystal devices. The electrical properties of the π-deficient quinones shown below were measured from vacuum-deposited thin film transistors.

To fabricate thin film transistors, the π-deficient pentacenequinones were purified by the physical vapor transport technique[27] and then deposited by thermal evaporation onto silicon wafers. The devices had gold as top-contact source and drain electrodes and highly doped Si as a gate electrode. A 300 nm-thick layer of SiO_2 that was modified with a self-assembled monolayer of octadecyltrimethoxysilane (OTMS)[28] functioned as dielectrics. In these devices, all the π-deficient pentacenequinones except **6** performed as n-type semiconductors with field effect. Listed in Table 2 is the electron mobility of each quinone as measured under vacuum. Characterization of thin film transistors of the quinones is detailed in the Supporting Information. Shown in Figure 7 are the output and transfer *I*−*V* curves for the best performing transistor of **3**. From the transfer *I*−*V* curve, a field-effect mobility of 0.18 cm^{2}V^{-1}s^{-1} is measured in the saturation regime using the equation: $I_{DS} = (\mu W C_i / 2L)(V_G - V_T)^2$ and C_i of 11nF/cm^2 for 300 nm SiO_2. The on/off ratio of the drain current obtained between 0 and 70 V gate bias is greater than 1×10^6. When the transistor of **3** was tested in the ambient air, the measured electron mobility decreased to 1×10^{-3} cm^{2}V^{-1}s^{-1}.

To understand why **3** and **5** have significantly higher mobilities than those of others, the thin films of all the quinones were studied with X-ray diffraction and atomic

(28) Ito, Y.; Virkar, A. A.; Mannsfeld, S.; Oh, J. H.; Toney, M.; Locklin, A.; Bao, Z. *J. Am. Chem. Soc.* **2009**, *131*, 9396–9404.

Table 2. Electron Mobilities (μ_e) of π-Deficient Pentacenequinones Measured from Thin Film Transistors under Vacuum

	2	**3**	**4**	**5**	**6**	**7**
μ_e (cm^{2}V^{-1}s^{-1})	$2-6 \times 10^{-5}$	$0.04-0.18$	$1-2 \times 10^{-5}$	$0.05-0.12$	no FET	$2-6 \times 10^{-5}$
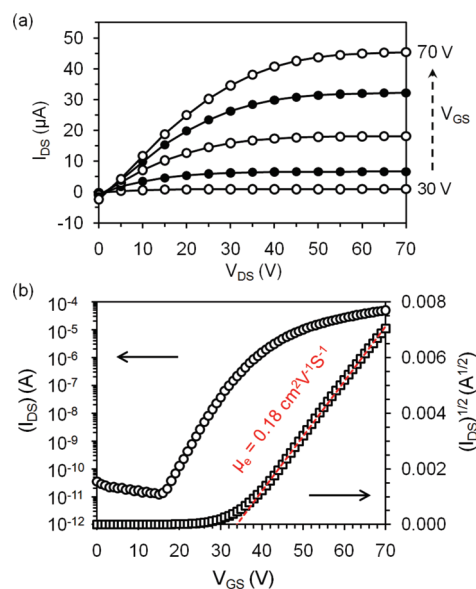
Figure 7. (a) Drain current (I_{DS}) versus drain voltage (V_{DS}) with varying gate voltage (V_{GS}) for a thin film transistor of **3** with the active channel of $L = 2$ mm and $W = 50$ μm. (b) Drain current (I_{DS}) versus gate voltage (V_{GS}) with drain voltage (V_{DS}) of 70 V for the same transistor of **3**.

force microscopy (AFM) as detailed in the Supporting Information. As indicated by the X-ray diffraction patterns,[29] **3** and **5** formed polycrystalline films, and the thin films exhibited polymorphs different from their bulk crystals.[30] In contrast, **2**, **4**, **6**, and **7** formed amorphous films as indicated by the absence of diffraction peaks. The poor performance of **2**, **4**, **6**, and **7** can, thus, be attributed to the amorphous nature of the films since it is well-known that the field effect mobility is very sensitive to the crystallinity of the thin film.[31] Because the field effect mobilities of the quinones reported here are limited by the film crystallinity, they cannot be related to the electronic structures and molecular packing to reach further conclusions on the structure–property relationship.

(29) The X-ray diffraction patterns of 3 are shown in the Supporting Information and those of **5** were reported in ref 5.
(30) XRD from the film of **3** shows three peaks at $2\theta = 9.10°$ (*d*-spacing: 9.71 Å), $2\theta = 18.49°$ (*d*-spacing: 4.80 Å), and $2\theta = 21.67°$ (*d*-spacing: 4.10 Å). In comparison, the first diffraction (002) derived from the single crystal structure of **3** appears at $2\theta = 12.10°$ (*d*-spacing: 7.31 Å).
(31) Dimitrakopoulos, C. D.; Malenfant, P. R. L. *Adv. Mater.* **2002**, *14*, 99–117.

Conclusions

In summary, detailed above is a comprehensive study on the synthesis, electronic structures, molecular packing, and n-channel thin film transistors of two groups of π-deficient pentacenequinones. It is found that both fluorine atoms and pyrazine-type nitrogen atoms are able to lower the LUMO energy level of pentacenequinone to yield n-type organic semiconductors. A comparison between the two groups of quinones in terms of their electronic structures and molecular packing has led to two interesting findings. First, The LUMOs of fluorinated pentacenequinones **2** and **3** have the same shape as that of **1** while the LUMOs of *N*-heteropentacenequinones **4**–**7** are of a different pattern. Second, although fluorinated quinone **3** and *N*-heteroquinones **5** and **7** have similar close π-stacking and quadruple weak H-bonds, the two types of quinones show an apparent difference in the relative shifts of π-stacked molecules along the molecular axes. The unusual quadruple C–H···N/O/F hydrogen bonds found from the crystal structures of **3**, **5**, and **7** may be applied as supramolecular synthons in crystal engineering.[24] Both of the two groups of quinones have been successfully applied as active components in n-channel thin film transistors with the field effect mobility up to higher than 0.1 cm^{2}V^{-1}s^{-1}. This suggests that π-deficient quinones would be a general design for n-type organic semiconductors. Further investigations on π-deficient quinones for applications not only in n-channel thin film transistors but also in organic solar cells are in progress in our laboratory.

Supporting Information Available: Syntheses and characterizations of **2**, **3**, **4**, **6** and **7**, thin film characterization with AFM and XRD, device fabrication and characterization, and the crystallographic information files for **3** and **7** (PDF, CIF). This material is available free of charge via the Internet at http://pubs.acs.org.